NUMERICAL SIMULATION OF TURBULENT FLOW IN A CYLINDRICAL CONTAINER UNDER ALTERNATING ROTARY MOTION

Roger Schipmann Eger, rogerseger@yahoo.com
César José Deschamps, deschamps@polo.ufsc.br
POLO – Research Laboratories for Emerging Technologies in Cooling and Thermophysics
Department of Mechanical Engineering
Federal University of Santa Catarina
88040-900, Florianópolis, SC, Brazil

Abstract. *Cylindrical container under rotary motion is widely used in several industrial applications, such as chemical and petrochemical, metallurgical, pharmaceutical, food and even for wastewater treatment. In some of these applications, the development of new products and materials commonly comprises mixing processes, which take advantage of rotational flow effects to reduce non-uniformities in composition, temperature and other properties. However, the complexity of the resulting flow field implies that most of the research related to this area is usually intended to the establishment of empirical correlations for specific applications. The lack of a detailed physical understanding of these flows turns the design of optimal systems and products into a very difficult task. This paper reports the results of a numerical simulation of turbulent flow in a cylindrical container under alternating rotary motion, with an impeller at the bottom surface. Experimental results are also obtained to complement the study and to validate the numerical model. The main physical phenomena involved are analyzed with reference to results for velocity, turbulence quantities and instantaneous torque.*

Keywords*: Rotating free surface flow, turbulence modeling, rotating container.*

1. INTRODUCTION

Swirling flows are widely used within a broad variety of industries, such as chemical and petrochemical, metallurgical, polymer, paper, pharmaceutical, food industry and even wastewater treatment. In fact, the development of new products and materials by these industries commonly comprises mixing processes, which are mostly employed to reduce non-uniformities in composition, temperature and other properties. In fact, an optimized mixing process can reduce time and costs involved.

Even though these processes are widely used, the complexity of the flow inside reactors and stirred tanks is such that most of the related research is only intended to the establishment of empirical correlations. These experimental studies are able to provide useful data about the mixing quality as a function of the mixer geometric parameters, but which are at the same time too specific and unable to provide a better understanding of the main physical phenomena involved in the process. In fatc, the lack of a detailed physical comprehension of such flows turns the design of optimal systems and products into a very difficult task.

According to Harnby *et al.* (1992), Alvarez *et al.* (2002) and Lackey (2004), the United States of America alone spend approximately 10 billion dollars per year with inefficient mixing processes. As mentioned before, the largest industrial application of rotary flows is the mixing processes.

Aubin *et al.* (2004) numerically analyzed the effect of modeling parameters in the following flow properties: mean velocity, turbulent kinetic energy, as well as global quantities, such as circulation and power number. Their analysis was performed for a baffled cylindrical vessel with a 6-blade-turbine and the working fluid was water. Results were validated with the assistance of LDA measurements, indicating that first order discretization schemes tend to underestimate significantly the experimental data, especially of turbulent kinetic energy.

Considering that reliable values of the turbulent energy dissipation, ε, is of great importance for the optimization of mixing processes, Baldi *et al.* (2004) developed an experimental strategy to obtain these values through direct measurement of the fluctuations of velocity gradients in the definition of ε. The study considered a cylindrical reservoir with a six-blade Rushton turbine, with measurements being performed with particle image velocimetry (PIV). The results were found to be in good agreement with several other data available in the literature. Studies about the accuracy of numerical results for dissipation of turbulent kinetic energy are very unusual in the literature. According to Baldi *et al.* (2004), simulations carried out with RANS based turbulence models often underestimate the levels of ε by up to 50%, while the use of large-scale simulation (LES) allows a more accurate estimate, although but computationally more expensive.

Montante *et al.* (2005) conducted a comparative study with the aim of identifying the potential of two CFD commercial codes in the prediction of mixing time through homogenization curves. The authors used the RNG k-ε turbulence model and pointed out that a critical point in the modeling is the choice of the turbulent Schmidt number, σ_t,. The turbulent Schmidt number is used to compensate the uncertainty in predicting the turbulent viscosity, μ_t, which is responsible for turbulent transport. The numerical results showed a very good agreement with experimental data for all

fluids considered in the study. Yeoh *et al.* (2005) carried out a similar work, but using LES to evaluate the turbulent flow.

Dular *et al.* (2006) simulated a non-Newtonian fluid flow, induced by a six-blade propeller in a cylindrical tank. The main objectives were to determine the shapes of the vortex under the blade and the free surface between the two phases, as well as the velocity field. The validation of the model was made possible with LDA measurements, in which the numerical results were shown to be consistent with the experimental data. Recently, Kumaresan *et al.* (2006) investigated the influence of various types of blade geometries on the efficiency of mixers, based on results for velocity, turbulent kinetic energy, maximum dissipation of turbulent kinetic energy, average strain rate and Reynolds normal stresses.

Savreaux *et al*. (2007) numerically analyzed the flow in a cylindrical tank used for mixing of viscoplastic fluids. Their main objective was to show effects of fluid plasticity that occasionally generate rigid areas, impairing the process of mixing and increasing energy consumption. In their two-dimensional analysis, the authors assessed the mixing performance through particle tracking.

The present paper reports a numerical analysis of turbulent flow in a cylinder tank, with triangular bumps on its bottom surface, subjected to an alternating rotary motion. The main objective is to investigate some of the main physical mechanisms that affect this fluid flow phenomenon, with reference to results for turbulence kinetic energy and its dissipation. The influence of the number of bumps assembled on the tank bottom is also addressed. Numerical prediction of the torque associated with the flow is compared with experimental data in order to validate the model.

2. MATHEMATICAL MODEL

This chapter presents very briefly the fundamental equations used to mathematically model the flow. First the equations of continuity and momentum are shown, and then details of the SST k-ω turbulence model employed in the study is detailed.

2.1. Continuity and Momentum

The law of conservation of mass for an incompressible flow can be represented by

$$\frac{\partial U_i}{\partial x_i} = 0 \tag{1}$$

where U_i is the velocity component in the xi direction.

The rate of change of linear momentum of a portion of fluid is equal to the resulting force which acts on the fluid. Assuming the hypotheses of Newtonian fluid and incompressible flow leads to the following form of the Navier-Stokes:

$$\frac{\partial}{\partial t}(\rho U_i) + \frac{\partial}{\partial x_j}(\rho U_i U_j) = \frac{\partial T_{ij}}{\partial x_j} + \rho f_i \tag{2}$$

where ρ stands for the specific mass, f_i represents de body forces per unit volume and T_{ij} is the Cauchy tensor.

2.2. Turbulence Model

As proposed by Reynolds in 1895, the instantaneous velocity of a fluid can be expressed as the sum of a mean velocity $\overline{U}$ and a turbulent fluctuation u':

$$U_i = \overline{U_i} + u_i' \tag{3}$$

By replacing Eq.(3) into Eq. (2), one obtains the Reynolds averaged Navier-Stokes equations (RANS), which can be written as follows:

$$\frac{\partial \rho}{\partial t} + \frac{\partial}{\partial x_i}(\rho \overline{U}_i) = 0 \tag{4}$$

$$\frac{\partial}{\partial t}(\rho \overline{U}_i) + \frac{\partial}{\partial x_j}(\rho \overline{U}_j \overline{U}_i) = -\frac{\partial p}{\partial x_i} + \frac{\partial}{\partial x_j}\left[\mu\left(\frac{\partial \overline{U}_i}{\partial x_j} - \rho\overline{u_i' u_j'}\right)\right] + \rho f_i \tag{5}$$

with the slashes over the symbols denoting averaged quantities. When using such average quantities, all information about the instantaneous fluctuations is lost. On the other hand, six new variables, $\overline{u_i' u_j'}$, are created, which are commonly referred as the Reynolds stresses. The presence of the Reynolds stresses leads to the well known closure problem, since the number of equations is smaller than the unknowns. In order to circumvent this problem, a turbulence models are needed to evaluate the Reynolds stresses.

In the present analysis, a turbulence model based on the eddy viscosity concept is used. With this purpose, the SST turbulence model was chosen, which is a hybrid formulation that adopts the k-ω model near solid walls and the k-ε model in the free stream.

The equation for k and ω are the following:

$$\frac{\partial(\rho k)}{\partial t} + \frac{\partial}{\partial x_j}\left(\rho \overline{U}_j k\right) = \frac{\partial}{\partial x_j}\left[\left(\mu + \frac{\mu_t}{\sigma_{k3}}\right)\frac{\partial k}{\partial x_j}\right] + P_k - \beta' \rho k \omega \tag{6}$$

$$\frac{\partial(\rho \omega)}{\partial t} + \frac{\partial}{\partial x_j}\left(\rho \overline{U}_j \omega\right) = \frac{\partial}{\partial x_j}\left[\left(\mu + \frac{\mu_t}{\sigma_{\omega 3}}\right)\frac{\partial \omega}{\partial x_j}\right] + (1 - F_1) 2\rho \frac{1}{\sigma_{\omega 2}\omega}\frac{\partial k}{\partial x_j}\frac{\partial \omega}{\partial x_j} + \alpha_3 \frac{\omega}{k} P_k - \beta_3 \rho \omega^2 \tag{7}$$

The coefficients of the model are a linear combination of the corresponding coefficients of the k-ω and k-ε models. Accordingly, F_1 is equal to 1 at the walls and 0 in the free stream, which is the requirement to obtain the k-ω model near the walls and the k-ε model in the free stream. This can be achieved through the following relationship:

$$F_1 = tanh\left[mín\left(máx\left(\frac{\sqrt{k}}{\beta' \omega y}, \frac{500\nu}{y^2 \omega}\right)\frac{4\rho k}{CD_{k\omega}\sigma_{\omega 2} y^2}\right)\right]^4 \tag{8}$$

where y is the distance to closest wall and

$$CD_{k\omega} = máx\left(2\rho \frac{1}{\sigma_{\omega 2}\omega}\frac{\partial k}{\partial x_j}\frac{\partial \omega}{\partial x_j}, 10^{-10}\right) \tag{9}$$

The constants present in the baseline k-ω model are listed in the Tab.1 (ANSYS CFX, 2006).

Table 1 - Coefficients of BSL k-ω model

β'	α_1	β_1	σ_{k1}	$\sigma_{\omega 1}$	α_2	β_2	σ_{k2}	$\sigma_{\omega 2}$
0,09	0,556	0,075	2	2	0,44	0,0828	1	1,168

As indicated by Menter (1993), both the k-ε model and the k-ω model neglect the transport of turbulent shear stress, leading to an over prediction of eddy-viscosity that make it difficult to predict flow separation along smooth surfaces. In order to get around this problem, the SST model adopts a formulation for the eddy-viscosity in which the presence of a limiter avoids its over estimation.

$$\nu_t = \frac{a_1 k}{máx(a_1 \omega, SF_2)} \tag{10}$$

where F_2 is a function used to restrict the limiter to the wall boundary layer:

$$F_2 = tanh\left[máx\left(\frac{2\sqrt{k}}{\beta' \omega y}, \frac{500\nu}{y^2 \omega}\right)\right]^2 \tag{11}$$

3. NUMERICAL SOLUTION PROCEDURE

Numerical simulation methods are nowadays one of the most effective alternatives for solving fluid flow. Among these methods are the finite element method (FEM) and finite volume method (FVM). In both cases the domain of interest is subdivided into a number of small volumes, called finite elements or control volumes, depending on the chosen approach. The quantities of interest are then calculated in an approximate manner in each of these volumes. Currently, the FEM is preferred for the solution of structural problems while the FVM reigns virtually absolute to simulate fluid flow.

The advantage of the finite volume method in relation to other methods in the solution of problems involving fluid flow are its conservative characteristics, which arise from the fact that the discretized equations are obtained through balances in the elementary volumes. In this study, the finite volume method was employed by means of the commercial code ANSYS CFX Release 11.0.

Truncation errors in the numerical results were verified through tests of time and grid discretizations. The meshes finally chosen has the best tradeoff relation between accuracy and computational processing time, with.the element next to the wall having a typizal dimension of 1 mm. Figure 1 gives a global view and zoomed view of the final grid.

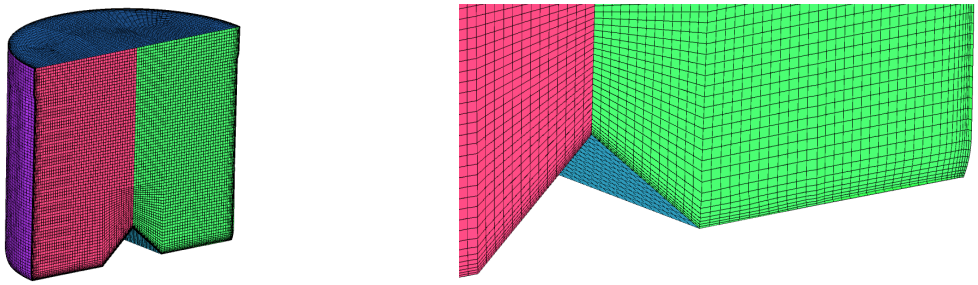

Figure 1. Computational mesh used in the simulations.

In order to spatially interpolate flow quantities, a high-order accurate scheme was chosen, whereas a first-order backwards Euler scheme was used for time interpolation. The commercial code ANSYS CFX uses a non-staggered grid layout so that the control volumes are the same for all transport equations. To avoid the decoupling of pressure and velocity fields, momentum-like equations are applied at the interfaces. The resulting systems of algebraic equations are solved with a coupled solver.

The formulation adopted herein for the flow includes centrifugal and Coriolis forces and, therefore, two extra terms are added to the source term of the momentum equations. The presence of a free surface of water in contact with air was described by a homogeneous multiphase model. The procedure used in the solution of multiphase flow through the homogeneous model is similar to that used in single-phase flows, with the inclusion of some terms due to the additional phases. It was considered no mass transfer between air and water, so that the volume of fluid technique could resolve and identify the interface between the fluids. The ANSYS CFX solver uses the Single Line Interface Construction (SLIC) algorithm for this task.

A first set of transient simulations was done in order to provide information about the influence of the tank rotational speed on the velocity field and torque. This first set of simulations was also used to validate the numerical model. Due to the symmetry characteristic of the reservoir, it was necessary to mesh and solve only one half of the domain as shown in Fig.1. Table 2 contains the boundary conditions that were applied to the solution domain.

Table 2 – Boundary Conditions

Boundary	**Boundary Condition Applied**
Sidewalls	Wall – No slip
Bottom	Wall – No slip
Top	Wall – Free slip
Symmetry plane	Rotational periodicity

The domain was set to a transient rotation following the curves shown in Fig.2. The time step adopted for all the analyses was 0.01 s. According to Fig. 2, the period of one cycle corresponds to 5.2 seconds, resulting therefore a total of 520 time steps per cycle. All simulations were run on a cluster with 2.33GHz Intel Xeon Quad-Core processors. The simulation was carried out by using parallel processing on a 75,000 elements per processor basis. A mesh with 220,000 volumes took approximately 38 hours per cycle. The simulations took 3 cycles to reach a fully periodic condition.

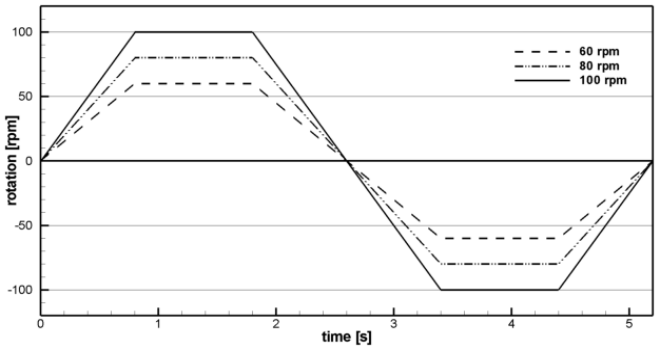

Figure 2. Rotation curves imposed to domain

4. RESULTS

4.1. Experimental Set-up and Validation Procedure

In order to validate the numerical results, an experimental set-up was adopted. It was composed by a cylindrical reservoir with a triangular bump attached to its bottom and a simple acquisition system. The tank was driven by a servo-motor, as shown in Fig.3.

Initially, the empty tank was put into rotation, with instantaneous rotation and torque data being acquired. Then, the tank was filled with 60 liters of water and measurements were performed once more. With these two sets of data, it was possible to evaluate the torque amount associated with the flow resistance.

The experiment was repeated three times for each one of the tank rotation curves shown in Fig.2. As can be seen in Fig. 4, good agreement was found when numerical results were compared with the experimental data for torque. It should be noticed that the oscillations that appear in the experimental results at 2 and 4.7 s are due to noise from the servo-motor control electronics.

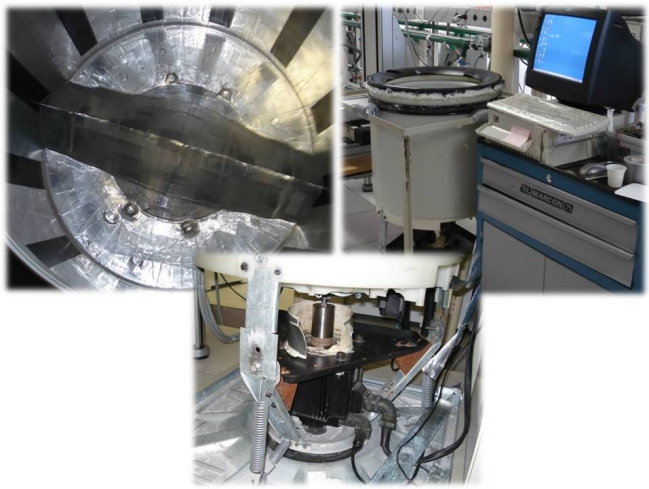

Figure 3. Experimental set-up

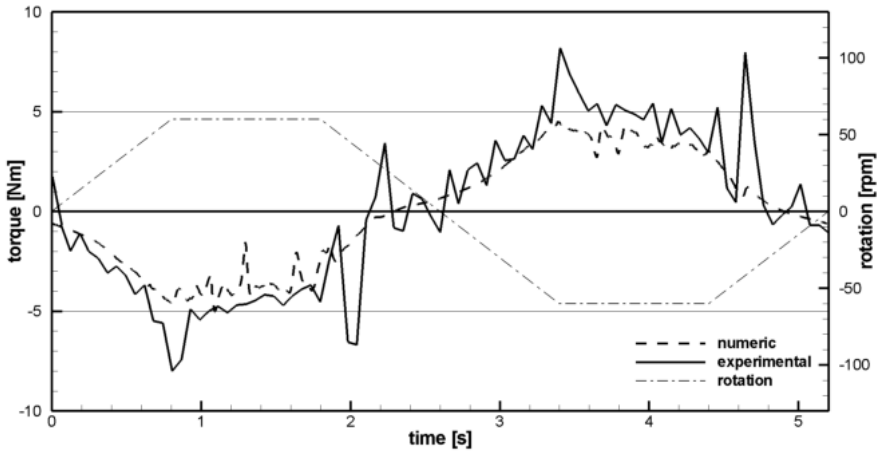

(a)

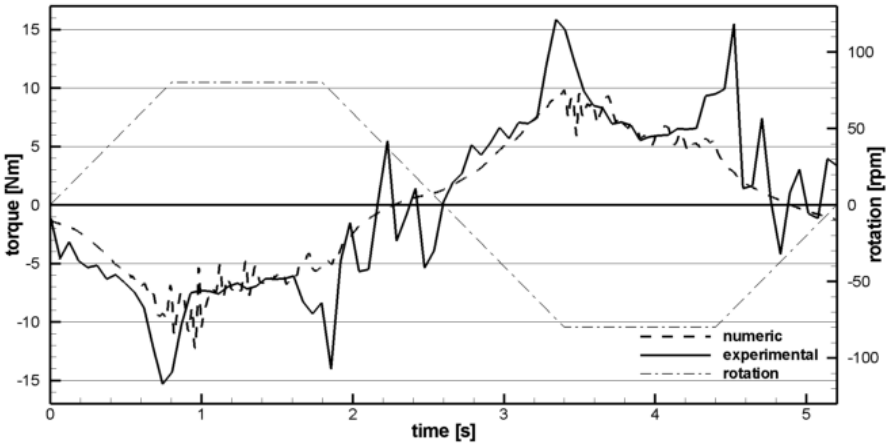

(b)

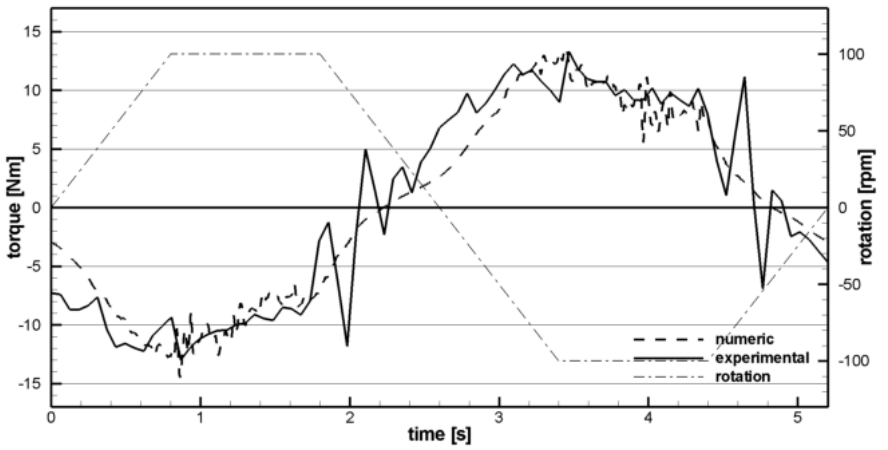

(c)

Figure 4. Experimental and numerical results for torque: (a) 60 rpm; (b) 80 rpm; (c) 100 rpm

Since the torque is calculated from the flow field, the aforementioned agreement is an indication that it was correctly predicted. The next set of simulations was used to analyze the effects of geometry on the flow, considering only the 100 rpm-amplitude-rotation profile.

4.2. Flow Analysis

Because of its inherent energy and mass transfer mechanisms, turbulence plays a key role in most mixing processes. In this respect, perhaps one of the most important quantities is the turbulent kinetic energy dissipation, ε, because it can be used as a reference parameter for optimization of mixing processes in terms of energy consumption. In other words, with these data in hand, it is possible to predict beforehand whether a system will consume more energy than another. Figure 5 shows results for the turbulent kinetic energy dissipation over a complete cycle of two geometries, one with two bumps and other with four bumps. As can be seen, dissipation is greater when two bumps are employed. Moreover, it can be noticed that the peak of eddy dissipation occurs at the time instant of 1.2 s for both geometries. Figure 6 shows the turbulence kinetic energy dissipation field at this very instant for the two geometries being analyzed.

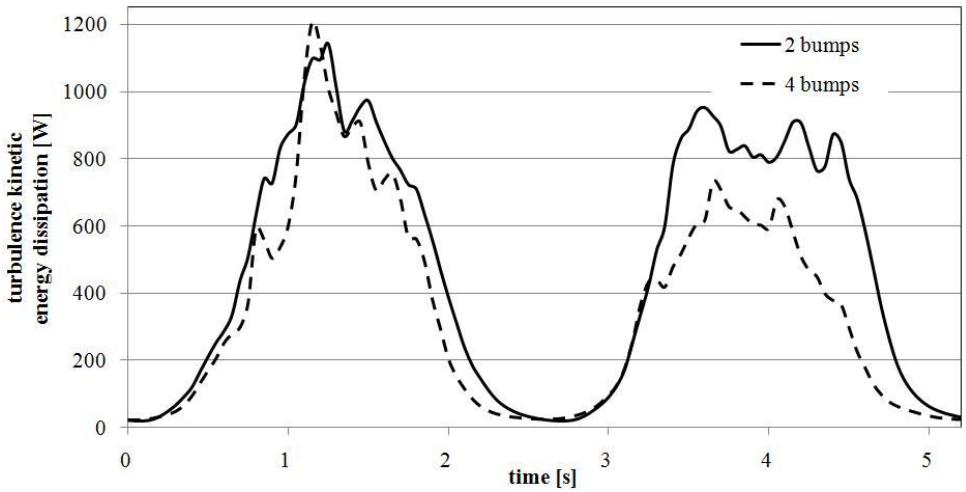

Figure 5. Total eddy dissipation over a cycle for two geometries.

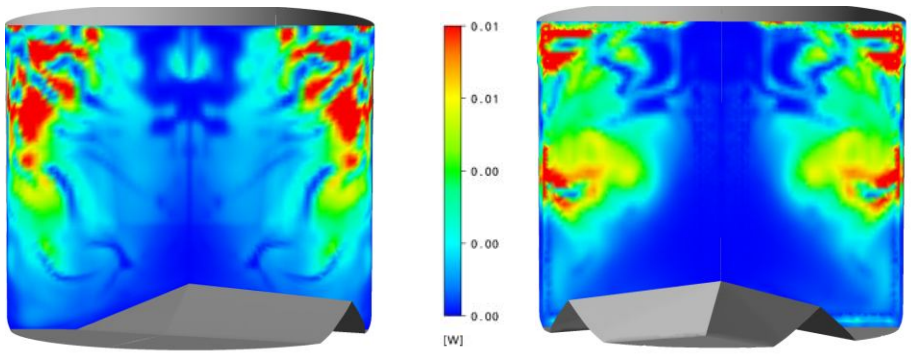

Figure 6. Instantaneous turbulence kinetic energy dissipation field at 1.2 s: (a) 2 bumps; (b) 4 bumps

Another interesting property to consider in the analysis is the turbulence kinetic energy, *k*, which is a measure of the kinetic energy of the turbulent motion. Therefore, high levels of this property usually mean a better performance for the mixing process, since turbulence acts to enhance diffusion in the flow.

Figure 7 shows the profile of the total turbulence kinetic energy over a complete cycle. It is clear that the 2-bump-configuration transfers more energy to the turbulence scales than the 4-bump configuration, which is not a trivial result. Although the higher levels of turbulent kinetic energy for the two-bump configuration, Fig. 8 indicates that the torque necessary to induce the flow is predominantly higher for the 4-bump configuration. Consequently, the energy consumption is lower for a 2-bump design, consuming 313 J per cycle, in comparison with 429 J for the 4-bump configuration.

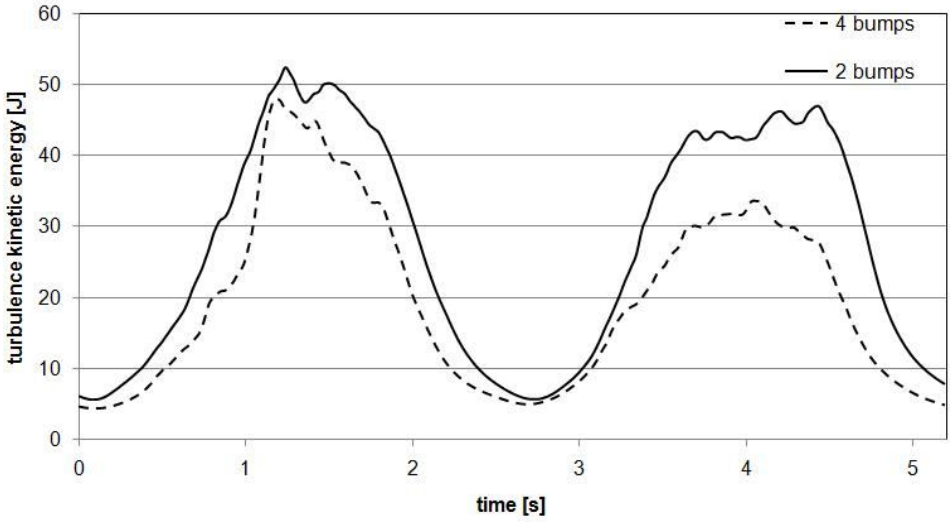

Figure 7. Total turbulence kinetic energy over a cycle: (a) 2 bumps; (b) 4 bumps.

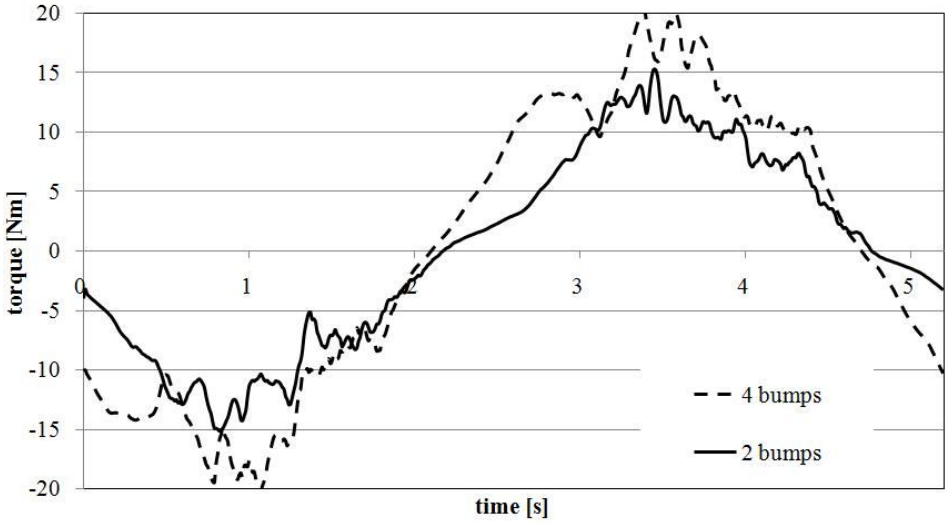

Figure 8. Flow resistance torque over a cycle: (a) 2 bumps; (b) 4 bumps.

Figure 9 was prepared to offer a view of the flow turbulence levels at five time instants along the period of one cycle. It is possible to identify whether the mixing, associated with turbulence kinetic energy, is well distributed in the tank or not.

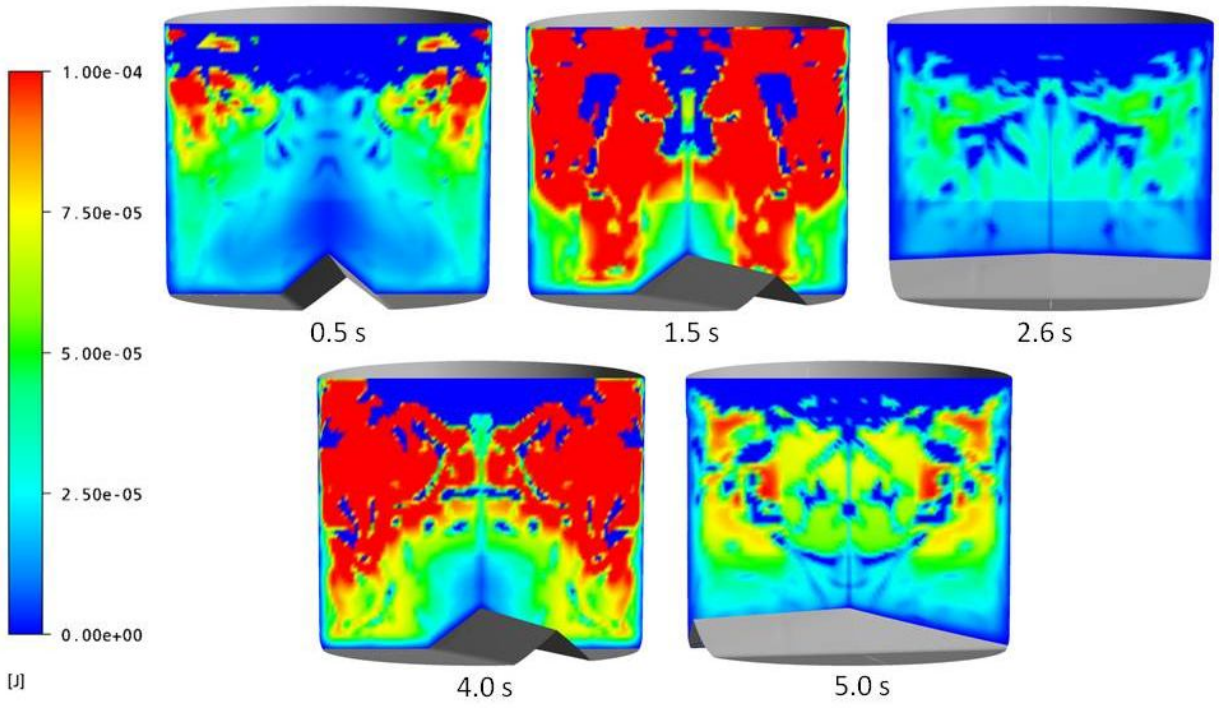

(a)

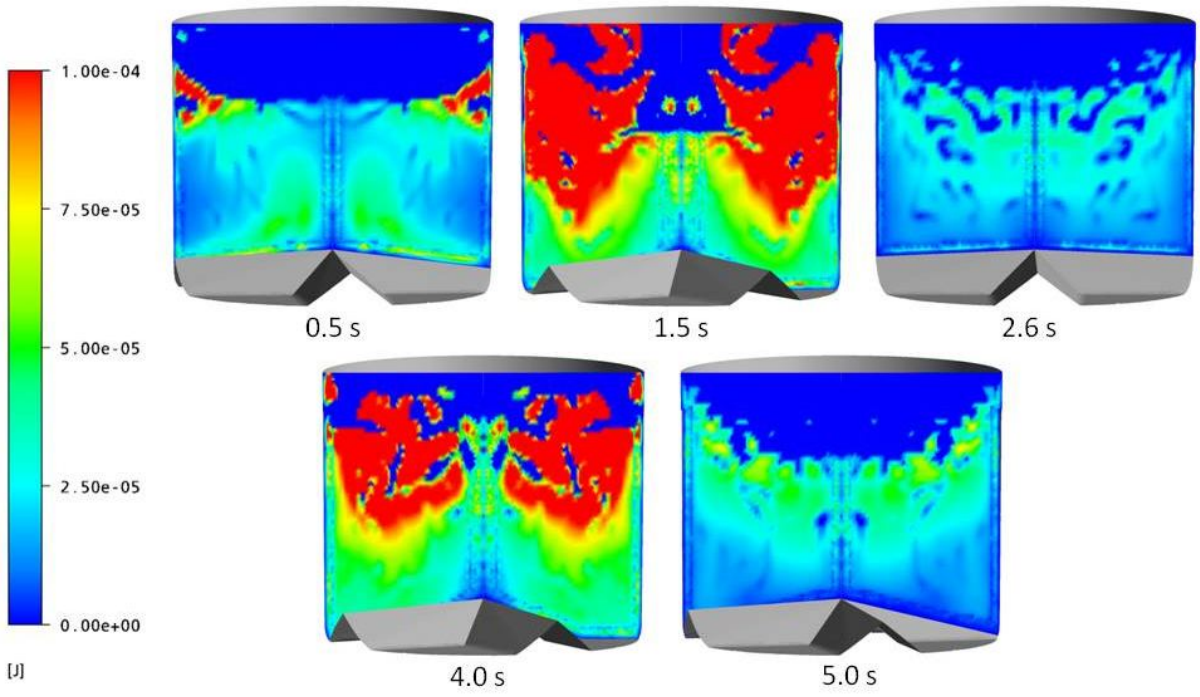

(b)

Figure 9. Turbulence kinetic energy field at different time instants: (a) 2 bumps; (b) 4 bumps.

5. CONCLUSIONS

A numerical model was developed to simulate turbulent flow in a cylindrical container under alternating rotary motion provided by an impeller at the bottom surface. Numerical results for flow resistive torque were shown to be in good agreement with experimental data obtained for three different flow conditions. It has been observed that turbulence kinetic energy and its dissipation are greater in tanks with 2 bumps than with 4 bumps. However, the torque necessary to induce the flow was predicted to be lower in the case of 2 bumps. Transient results for turbulence kinetic energy were analyzed at five time instants along the period of one cycle, allowing the identification of the better tank configuration for mixing.

6. ACKNOWLEDGEMENTS

This study forms part of a joint technical-scientific program of the Federal University of Santa Catarina and Electrolux do Brasil S.A.. Support from CNPq (Brazilian Research Council) is also acknowledged.

7. REFERENCES

ANSYS, Inc., "ANSYS CFX-Solver theory guide", Release 11.0, USA, 2006.

AUBIN, J., FLETCHER, D. F., XUEREB, C., Modeling turbulent flow in stirred tanks with CFD: the influence of the modeling approach, turbulence model and numerical scheme, Experimental Thermal and Fluid Science, Vol. 28, pp 431 – 445, 2004.

BALDI, S., YIANNESKIS, M., On the quantification of energy dissipation in the impeller stream of a stirred vessel from fluctuating velocity gradient measurements, Chemical Engineering Science, Vol. 59, pp 2659 – 2671, 2004.

DULAR, M., BAJCAR, T., SLEMENIK-PERŠE, L., ŽUMER, M., ŠIROK, B., Numerical simulation and experimental study of non-newtonian mixing flow with a free surface, Brazilian Journal of Chemical Engineering, Vol. 23, pp. 473 – 486, 2006.

KUMARESAN, T., JYESHTHARAJ, B., Effect of impeller design on the flow pattern and mixing in stirred tanks, Chemical Engineering Journal, Vol. 115, pp 173 – 193, 2006.

LACKEY, T. C., Numerical Investigation of Chaotic Advection in Three-Dimensional Experimentally Realizable Rotating Flows, Tese de Doutorado em Engenharia Civil e Ambiental, Departamento de Engenharia Civil e Ambiental, Instituto de Tecnologia da Geórgia, Geórgia, 2004.

MENTER, F.R., "Zonal two equation k-ω turbulence models for aerodynamic flows", AIAA Paper 93-2906, 1993.

MONTANTE, G., MOŠTĚK, M., JAHODA, M., Magelli, F., CFD simulations and experimental validation of homogenization curves and mixing time in stirred Newtonian and pseudo plasticliquids, Chemical Engineering Science, Vol. 60, pp 2427 – 2437, 2005.

SAVREUX, F., JAY, P., MAGNIN, A., Viscoplastic fluid mixing in a rotating tank, Chemical Engineering Science, Vol. 62, pp 2290 – 2301, 2007.

VERSTEEG, H. K., MALALASEKERA, W., "An introduction to computational fluid dynamics, Longman Scientific & Technical", Nova York, 1995.

YEOH, S.L., PAPADAKIS, G., YIANNESKIS, M., Determination of mixing time and degree of homogeneity instirred vessels with large eddy simulation, Chemical Engineering Science, Vol. 60, pp 2293 – 2302, 2005.

8. RESPONSIBILITY NOTICE

The authors are the only responsible for the printed material included in this paper.